PREDICTING EXPLOSION-GENERATED *Sn* AND *Lg* CODA USING SYNTHETIC SEISMOGRAMS

Jessie L. Bonner, Anastasia Stroujkova, and Kevin M. Mayeda

Weston Geophysical Corporation

Sponsored by National Nuclear Security Administration

Contract No. DE-AC52-05NA26610
Proposal No. BAA05-59

ABSTRACT

Recent examinations of the characteristics of coda-derived *S* and *Lg* spectra for yield estimation have shown that the spectral peak of Nevada Test Site (NTS) explosion spectra is depth-of-burial dependent, and that this peak is shifted to higher frequencies for Lop Nor explosions at the same depths. To confidently use coda-based yield formulas, we need to understand and predict coda spectral shape variations with depth, source media, velocity structure, topography, and geological heterogeneity.

We are in the final year of a synthetic seismogram study to evaluate the characteristics of *Lg* coda generated from explosions and earthquakes. To meet our objectives, we have developed a deterministic model for the western United States and the NTS. In order to generate coda in our 2D and 3D pseudospectral simulations, heterogeneity was added in the crust and/or upper mantle. Three parameters—correlation length, Hurst number (H), and fractional velocity perturbation of the heterogeneities—are used to construct different realizations of random media. We have estimated the heterogeneity parameters for the NTS using available seismic and geologic data. Lateral correlation, variance and coherence measures between seismic traces are estimated from clusters of nuclear explosions and well-log data. The horizontal von Karman correlation length estimated for nuclear explosion *Lg* phases is between 0.4–1.1 km, with Hurst numbers between 0.3 and 0.6. A dominant heterogeneity dimension of 0.5–1.8 km results in best *Lg* coda coherence at frequencies between 1 and 4 Hz.

Examples of the *Lg* and *Lg* coda synthetics produced by these models resemble NTS earthquake and explosion waveforms; however, there is a considerable non-uniqueness problem that must be addressed. We investigated methods for quantifying our synthetics in order to assure that simulated waveforms have similar characteristics as observed coda and direct *Lg*. One such characteristic is that the Q estimates for direct *Lg* and its coda are typically observed to be near equivalent in many tectonic settings. For example, near the NTS, Q_{Lg} (direct) and Q_{Lg} (coda) typically range between 200–300. Thus, we have compared the Q values of synthesized *Lg* coda and direct *Lg* from models with different attenuation structures. These structures range from constant shear wave Q (e.g., Q_{β}=200 or 500) throughout the crust to published, depth-dependent models for the Basin and Range. We examined the effect of the location of the stochastic variations (e.g., within the entire crust, above the middle crust, or only in the upper crust) on the Q_{Lg} (direct) and Q_{Lg} (coda) estimates obtained from the synthetics. The comparison of the variations in Q estimates for different source types (e.g., earthquakes and explosions) at different depths suggests that our stochastic models produce realistic 1 Hz estimates of Q_{Lg} (direct) and Q_{Lg} (coda) for published Basin and Range attenuation models. Estimates for the frequency dependence of the synthetic coda are relatively high compared to observed data.

We are currently using these calibrated stochastic models to generate regional-distance synthetics for monopole explosions at depths ranging from 0.1 to 1 km for all test site models. We have superposed secondary source effects, such as a compensated linear-vector dipole (CLVD) source, on the monopole synthetics. We are now deriving *Sn* and *Lg* coda spectra from the synthetics, estimating moments and yields from these spectra, and comparing them to observed data from NTS. If successful, this synthetic method may be used to estimate the *S* and *Lg* coda properties for yield estimation of explosions at either historical test sites or for broad, uncalibrated regions where we will likely have little information on velocity structure.

Report Documentation Page

Form Approved
OMB No. 0704-0188

1. REPORT DATE	2. REPORT TYPE	3. DATES COVERED
SEP 2008		**00-00-2008 to 00-00-2008**

4. TITLE AND SUBTITLE	5a. CONTRACT NUMBER
Predicting Explosion-Generated SN and LG Coda Using Syntheic Seismograms	5b. GRANT NUMBER
	5c. PROGRAM ELEMENT NUMBER
6. AUTHOR(S)	5d. PROJECT NUMBER
	5e. TASK NUMBER
	5f. WORK UNIT NUMBER
7. PERFORMING ORGANIZATION NAME(S) AND ADDRESS(ES) **Westom Geophysical Corporation,181 Bedford St,Lexington,MA,02420**	8. PERFORMING ORGANIZATION REPORT NUMBER
9. SPONSORING/MONITORING AGENCY NAME(S) AND ADDRESS(ES)	10. SPONSOR/MONITOR'S ACRONYM(S)
	11. SPONSOR/MONITOR'S REPORT NUMBER(S)

12. DISTRIBUTION/AVAILABILITY STATEMENT
Approved for public release; distribution unlimited

13. SUPPLEMENTARY NOTES
Proceedings of the 30th Monitoring Research Review: Ground-Based Nuclear Explosion Monitoring Technologies, 23-25 Sep 2008, Portsmouth, VA sponsored by the National Nuclear Security Administration (NNSA) and the Air Force Research Laboratory (AFRL)

14. ABSTRACT
see report

15. SUBJECT TERMS

16. SECURITY CLASSIFICATION OF:			17. LIMITATION OF ABSTRACT	18. NUMBER OF PAGES	19a. NAME OF RESPONSIBLE PERSON
a. REPORT	b. ABSTRACT	c. THIS PAGE			
unclassified	**unclassified**	**unclassified**	**Same as Report (SAR)**	**10**	

OBJECTIVES

We are attempting to determine why the current mechanisms for *Sn* and *Lg* generation from explosions often produce stable coda magnitudes that are transportable between test sites. We aim to understand and predict *Lg* and *Sn* coda spectral shapes with variations in source depth, material properties, velocity structure, and geological heterogeneity.

Our investigation objectives include the following:

1) Compilation and parameterization of seismic velocity models consisting of deterministic material models with stochastic perturbations;

2) Estimation of the effect of deterministic and stochastic model parameters on *Lg* propagation using synthetic waveforms generated by the Generalized Fourier Method (GFM) (Orrey, 1995);

3) Calibration of stochastic variations at each test site using nearby earthquake data; and

4) Calculation of 2D/3D synthetics for composite explosion source models of varying depths and moments for each test site.

During the past year, we have worked on all four of our above objectives and are near completion of the project. If these methods prove to be successful for explaining the characteristics of explosion-generated direct *Lg* and *Lg* coda at the NTS, we plan to test the transportability of these modeling techniques at the Shagan, Degelen, Novaya Zemlya, and Lop Nor test sites.

RESEARCH ACCOMPLISHED

Modeling Direct *Lg* and *Lg* Coda Q in the Basin and Range

The objective of our research is to determine if numerical modeling of *Lg* and its coda can replicate the depth-dependent spectral peaking observed at the NTS (Murphy et al., in review). In order to complete this task, we have developed a velocity and attenuation model for the NTS and are currently calibrating the stochastic parameters of the model.

Velocity Model. The background deterministic velocity structure for NTS (Figure 1) is based on a regional model for the Basin and Range similar to the model developed by Benz et al. (1991). The velocities in the upper crust are based on borehole data, geologic and gravity data, refraction studies and seismic experiments (McLaughlin et al. 1983; Stump and Johnson, 1984; Ferguson et al., 1994; Stevens et al., 1991). We have used various techniques to estimate stochastic parameters for the Basin and Range. This includes using previous well-located nuclear explosions to estimate correlation lengths for scattering of the *Lg* phase (Tibuleac et al., 2005, 2006). These results suggest that the horizontal correlation (Ay) lengths for a von Karman stochastic model range between 0.5 - 1 km with smaller vertical correlation (Az) lengths. The H numbers are related to the fractal dimension of the medium and range between 0.3 and 0.6. Figure 1 shows the results of converting the deterministic velocity model for the NTS region into a stochastic model for generating direct *Lg* and its coda.

Attenuation Models. We have considered different intrinsic background attenuation models in our numerical modeling exercises, ranging from constant shear wave Q models to published Q models for the western United States. Bonner et al. (2007) measured Q_{Lg} (direct) and Q_{Lg} (coda) from synthetics propagated through a constant shear wave Q model (e.g., Q_β = 200 or 500) for the entire crust. Their modeling suggested that Q_{Lg} (direct) typically ranged between the values of Q_β and Q_a for models without stochastic variations. Stochastic variations lowered the apparent Q_{Lg} (direct); however, it was troubling that the measured Q_{Lg} (direct) and Q_{Lg} (coda) were never approximately the same. A comparison of regionalized Q maps often shows the near-equivalence of these two estimates of attenuation.

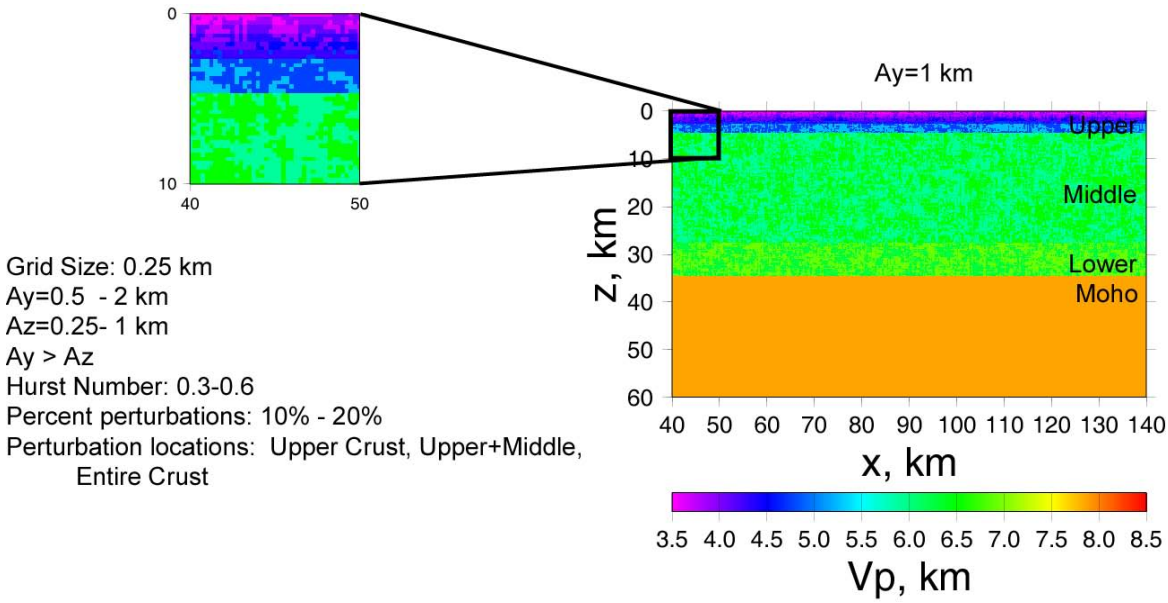

Figure 1. Example of a 2D stochastic model for the NTS used to model Q_{Lg} (direct) and Q_{Lg} (coda) in this study. Also listed are the variations in Ay, Az, Hurst number, and perturbation magnitude and location used to make different models for testing.

In this paper, we examine synthetics propagated through two published Q models for the Basin and Range. The Patton and Taylor (PT) (1984) model is characterized by low Q_β (85–172) throughout the entire crust. Similarly, the Mitchell and Xie (MX) (1994) model has low Q_β in the upper crust (50–80); however, they suggest high Q_β in the middle to lower crusts (400–1000). We incorporated these two Q models into our deterministic and stochastic models (Figure 1) for the NTS and computed synthetics for earthquakes using the GFM (Orrey, 1995).

Methodology. Record sections of GFM synthetic waveforms generated by four different perturbations of our NTS model are shown in Figure 2, including deterministic (e.g., without stochastic heterogeneity) and stochastic (Ax = 1, Az = 0.5) versions for both the PT and MX attenuation models. The appearance of the synthetics with stochastic variations compares favorably with observed waveforms from earthquakes and explosions in the Basin and Range (see Tibuleac et al., 2005, 2006 for additional examples).

Direct *Lg* Q Estimation. We windowed the direct *Lg* arrivals between 3.6 and 3.0 km/sec and estimated the spectral amplitudes A at each station at distance *R*. We used a cosine taper and smoothed the spectra in order to reduce the variance between the stations. For each frequency *f* we used the following equation (Mitra et al., 2006):

$$\log_{10} A + 0.5 \log_{10} R = \log_{10} S - \frac{\pi f \log_{10} e}{vQ} \qquad (2)$$

to solve for *Q(f).* For each frequency, we plotted $\log_{10}A + 0.5 \log_{10} R$ versus *R* and performed a linear regression to determine Q. We used a velocity (v) of 3.5 km/sec for the direct *Lg* arrival. Plots of the Q as a function of frequency are then used to estimate the Q at 1 Hz (Q_o) and the frequency dependence (η) (see Figure 3). Because of the grid size and velocities in our models, our simulations are only valid at frequencies less than 2–3 Hz.

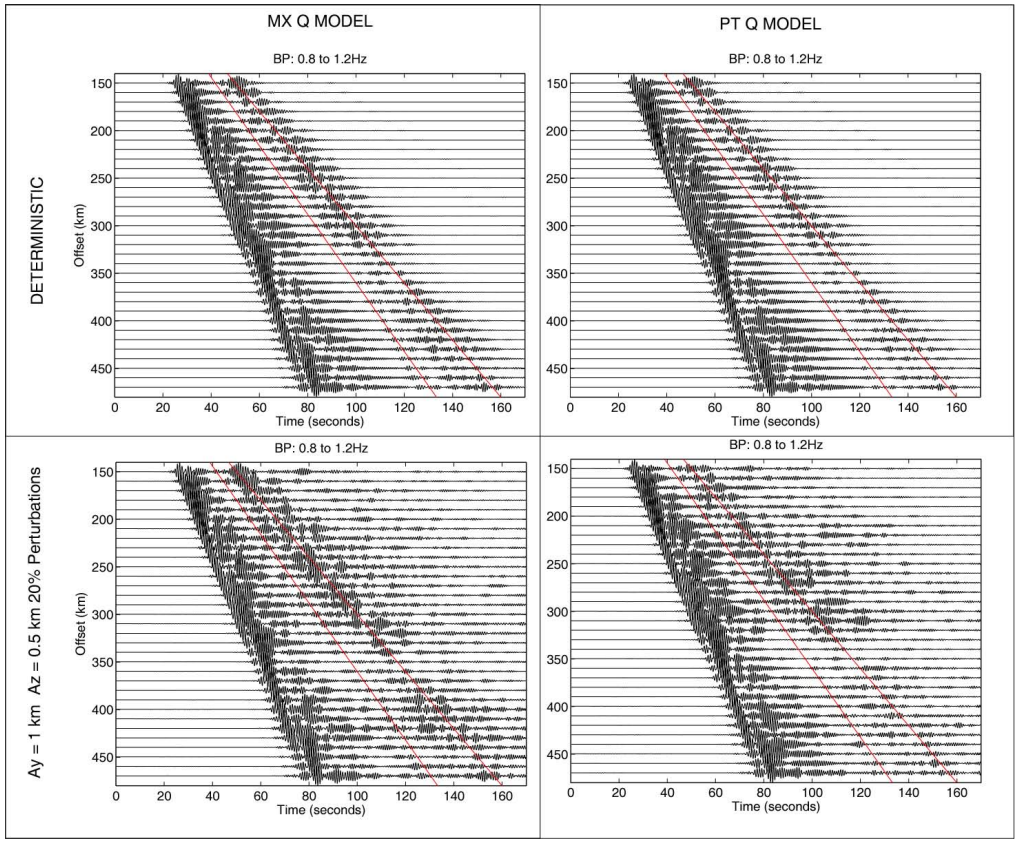

Figure 2. GFM Synthetic waveforms filtered near 1 Hz for deterministic (Top Row) and stochastic (Bottom Row) models for the NTS. Synthetics in the left column were propagated through the Mitchell and Xie (1994) Q model while the Patton and Taylor (1984) Q model was used to attenuate the synthetics in the right column.

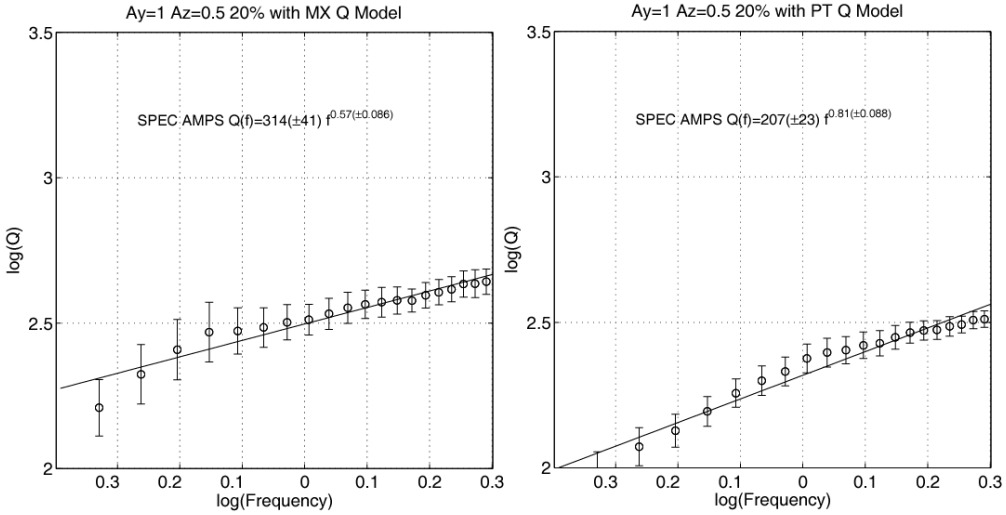

Figure 3. Estimating Q_{Lg} (direct) from synthetics. (Left) Regression of log Q versus frequency for *Lg* propagated through a stochastic NTS model with the Mitchell and Xie (1994) shear-wave Q model. (Right) Same as left except for use of Patton and Taylor (1984) Q model. There appears to be two different trends (above and below 1 Hz); however, for this study, we can fit most of the data plus error with a single line.

Given the non-uniqueness associated with synthetic modeling efforts similar to this, we decided to determine if our GFM synthetics have similar characteristics as observed coda and direct *Lg*. In the remaining sections, we compute the apparent Q_{Lg} (direct) and Q_{Lg} (coda) values for the synthetics using different Q models for comparison to observed estimates in the Basin and Range.

***Lg* Coda Q Estimation.** To estimate Q_{Lg} (coda) , we used the stacked spectral ratio (SSR) method of Xie and Nuttli (1988). In this method, amplitude spectra for windows at different times within the synthetic coda are used to form spectral ratios. The ratios are corrected for velocity and geometrical spreading, stacked, and regressed versus frequency to determine the coda Q at 1 Hz (Q_o) and the frequency dependence (η). Examples of the SSR analysis on synthetic data are shown in Figure 4.

Results. Table 1 provides measured Q_{Lg} (direct) and Q_{Lg} (coda) in the Basin and Range from previous studies. These results suggest that both the direct and coda Q for the *Lg* phase recorded in this region should range between 200-300 with η between 0.40 and 0.80. Table 2 and Figure 5 show the results of measuring the direct *Lg* Q and *Lg* coda Q for synthetics propagated through our different deterministic and stochastic models for the Basin and Range. Without the presence of stochastic variations, GFM synthetics in an XM Q model do not produce Q_{Lg} (direct) values that match the measured estimates for the Basin and Range. However, with 20% stochastic variations added to the model, the XM Q model produces synthetics with Q_{Lg} (direct) and Q_{Lg} (coda) that fall within the range of observed data. The synthetic Q_{Lg}s (direct) for all PT models were within the measured range; however, adding 20% variations resulted in Q_{Lg} (coda) estimates that were slightly below observed. Unfortunately, our synthetics do not reproduce the observed Q_{Lg} (coda) frequency dependence η no matter which Q model is used. In the coming months, we hope to determine the reason for this discrepancy, which could include the effects of using 2D versus 3D models as well as possible need for frequency-dependent intrinsic attenuation in the model.

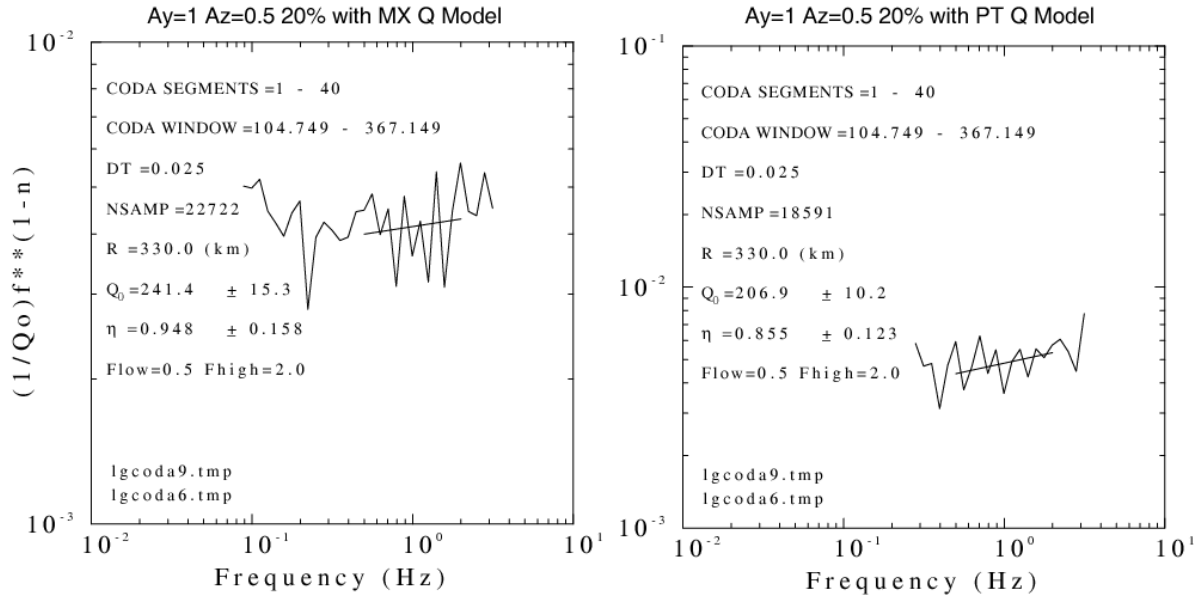

Figure 4. SSR method (Xie and Nuttli, 1988) applied to synthetic waveform data for *Lg* coda Q estimation for a stochastic model with Mitchell and Xie (left) and Patton and Taylor attenuation (right).

Table 1. Observed Q_{Lg} (direct) and Q_{Lg} (coda) for the Basin and Range

Q Study	Q_{Lg} (direct)	Q_{Lg} (coda)	*Lg* Q_o (direct)	η
Singh and Herrmann (1983)		200-300		0.40-0.60
Chavez and Priestley (1986)	214 ± 15			0.54
Xie and Mitchell (1990)	267 ± 56	275 ± 26		
Baqer and Mitchell (1998)		250-300		0.40-0.60
Benz et al. (1997)	235 ± 11			0.56 ± 0.04
Aleqabi and Wysession (2006)			234-312	0.40-0.80

Table 2. Synthetic Q_{Lg} (direct) and Q_{Lg} (coda) for Basin and Range models

	Q_{Lg} (direct)				Q_{Lg} (coda)				Stochastic Parameters			
MODEL	Lg Q_o	Error	η	Error	CODA Q_o	Error	η	Error	Q Model	Ay	Az	Percent
1	225	22	1	0.05	214	13	1.1	0.1	PT	1	0.5	10%
2	207	23	0.81	0.09	195	12	0.92	0.09	PT	1	0.5	20%
3	253	26	0.9	0.05	208	16	1.16	0.1	PT	1	0.25	10%
4	207	21	0.96	0.03	197	9	0.88	0.08	PT	1	0.25	20%
5	267	22	1.3	0.21	---	--	----	----	PT	---	----	---
6	385	51	0.69	0.04	263	25	1.11	0.11	XM	1	0.5	10%
7	314	41	0.57	0.07	237	20	0.84	0.11	XM	1	0.5	20%
8	370	59	0.98	0.07	251	20	1.17	0.1	XM	1	0.25	10%
9	310	31	1.1	0.06	233	13	0.91	0.1	XM	1	0.25	20%
10	632	127	1	0.05	---	--	----	----	XM	---	----	---

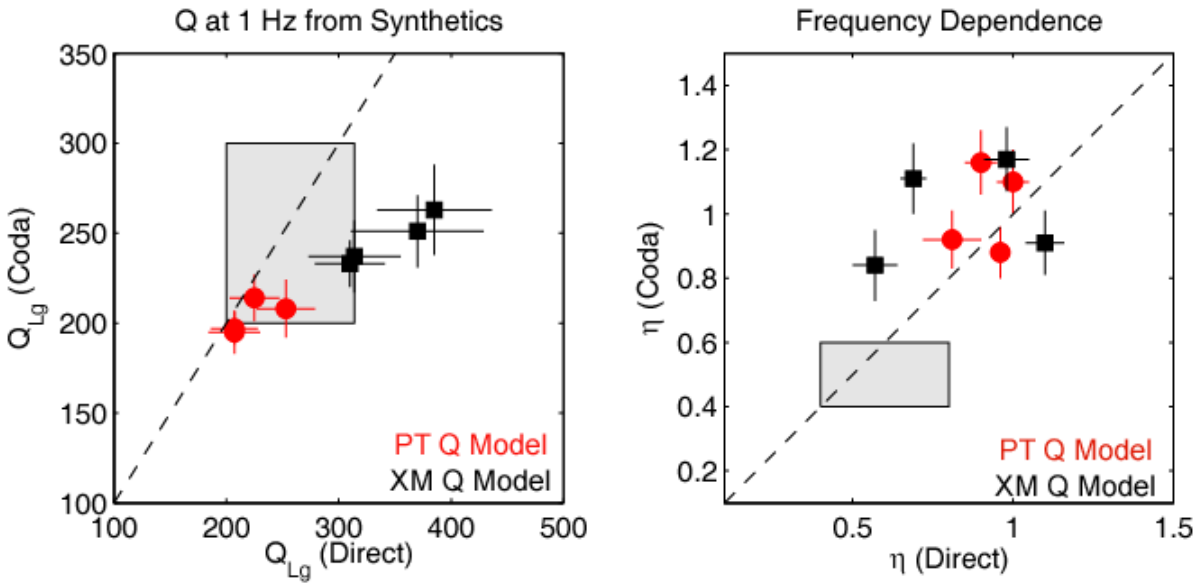

Figure 5. Q_o (left) and η (right) determined for *Lg* synthetics from Basin and Range stochastic models compared to observed estimates (shaded regions).

Modeling NTS Explosion-Generated Coda. The earthquake simulations using the Patton and Taylor (1994) Q model for the Basin and Range together with various stochastic perturbations provide Q_{Lg} (direct and coda) estimates that best match observed data (Table 2). We generated explosion synthetics for PT models 1-4 and

compared them to NTS nuclear explosions recorded at station MNV (distance ~230 km). Figure 6 shows a comparison of the MNV recordings of the NTS event Brie compared with synthetics for Model 1. Model 1 consists of the PT Q model and stochastic variations up to 10% with correlation distances of 1.0 to 0.5 km. The synthetics and observed data were normalized to their maximum *Pg* amplitudes. Brie was detonated a depth of less than 250 meters (Murphy et al., in review); therefore, we placed our monopole explosion source at a depth of 250 meters in order to compute the synthetics. The synthetics are valid at frequencies less than 2-3 Hz, and both the observed and synthetic waveforms in Figure 6 have been bandpass filtered between 0.1 and 2 Hz.

A quick glance of the waveforms in Figure 6a might suggest good agreement between the observed and synthetic arrivals. The *Pn* and *Pg* arrivals show very good correlation in both relative amplitude and arrival times. We note that the *Lg* arrival (green box) is not as pronounced in the synthetic waveform as it is in the observed data, and that the synthetic coda (blue box) has higher frequency content and more rapid amplitude decay than the observed data. This is also shown by the coda spectra in Figure 6b which shows a large amplitude peak near 0.9 Hz in the observed data that is missing from the synthetic coda.

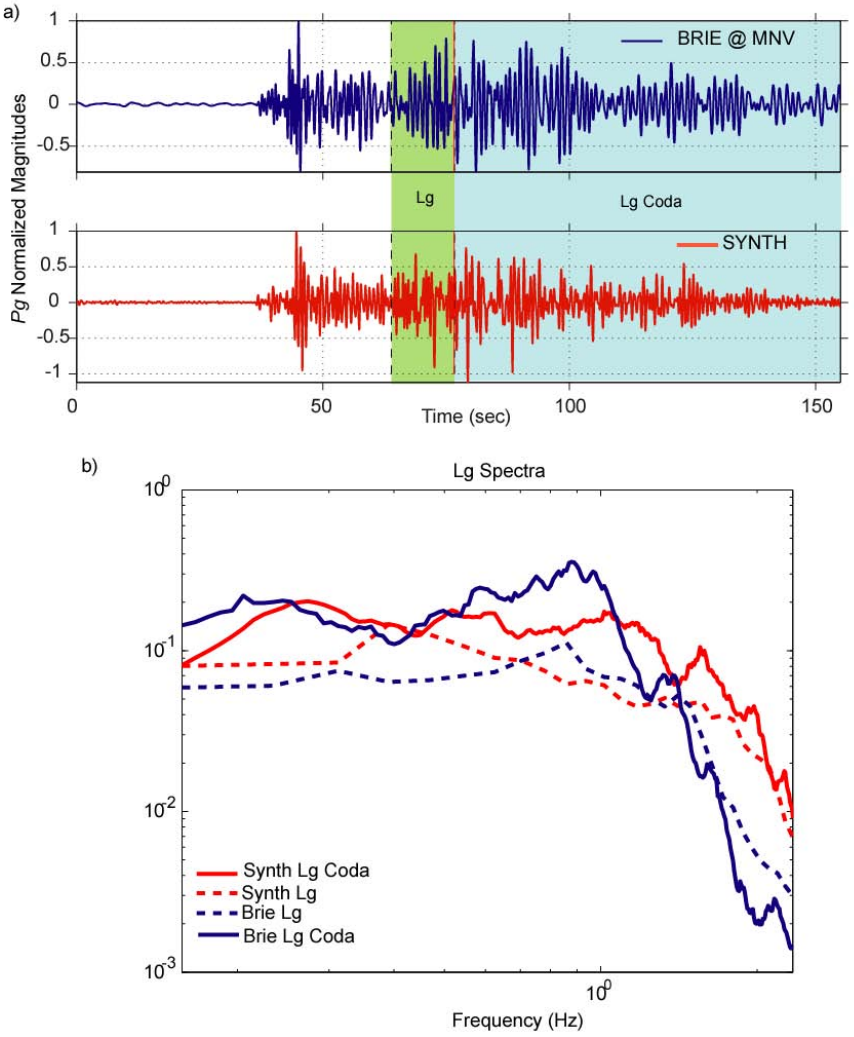

Figure 6. Explosion synthetics and data. a). Comparison of observed waveforms for the NTS explosion Brie recorded at NTS compared to GFM synthetics for the explosion using Model 1 from Table 2. The time windows for *Lg* and *Lg* coda (green and blue boxes, respectively) were used to compute spectra (b).

The correlation distances for the Model 1 perturbations were 1 and 0.5 km, and the results shown in Figure 6 suggest that coda energy at frequencies less than 1 Hz was being scattered too rapidly when compared to observed data. By decreasing the correlation distance from 0.5 to 0.25 km, we should decrease the rapid scattering below 1 Hz. This is confirmed in the seismograms and spectra for simulations using Model 4 (Figure 7). The simulations for Model 4 have increased energy near 1 Hz in the first 25 seconds of the coda analysis window compared to the synthetics shown in Figure 6. We note peaks in the synthetic and observed spectra between 0.9 and 1 Hz (Figure 7b). These synthetics provide an excellent comparison to the observed data for the *P*, *P* coda, direct *Lg*, and early coda arrivals. Our synthetics do not do an adequate job of modeling the observed coda at periods less than 0.7 Hz at onset times greater than 120 seconds (see Figure 8), which may be the result of reaching the limit of our 2D coda modeling methods. The later arriving coda may be multi-pathing from structures away from the direct path, which can not be effectively modeled using only 2D profiles. In the remaining months of the project, we will also add a CLVD source to the monopole explosion to see if the addition of more short-period surface-wave energy could improve the match between observed and synthetic coda.

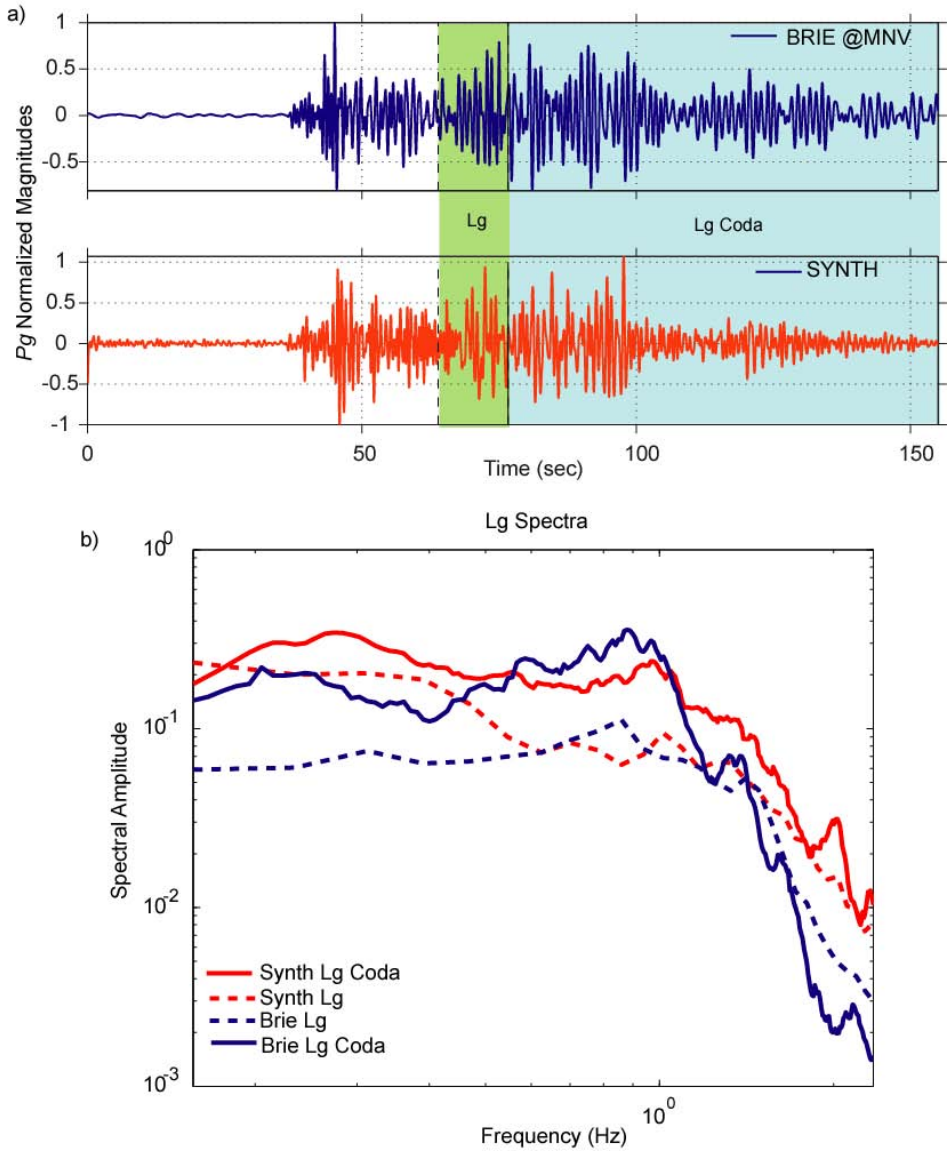

Figure 7. Explosion synthetics and data. a) Comparison of observed waveforms for the NTS explosion Brie recorded at NTS compared to GFM synthetics for the explosion using Model 4 from Table 2. The time windows for *Lg* and *Lg* coda (green and blue boxes, respectively) were used to compute spectra (b).

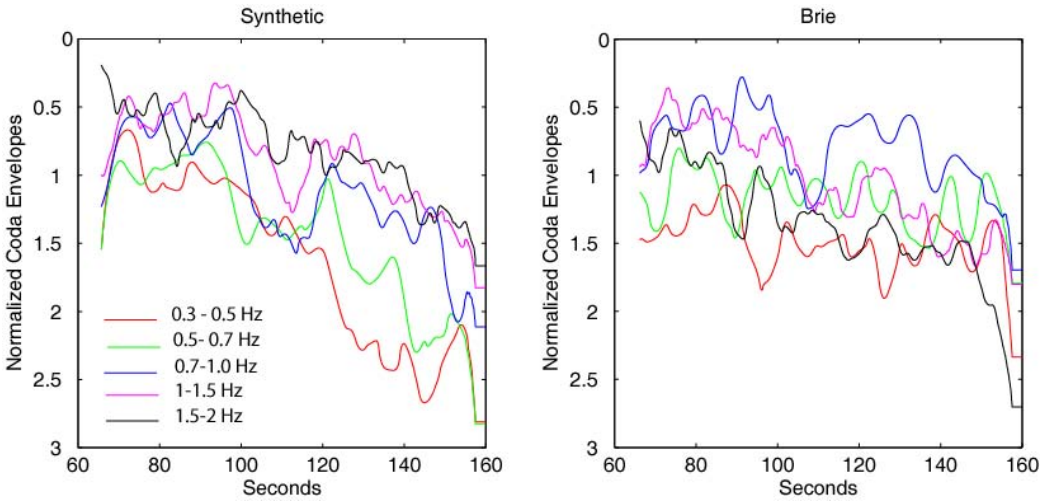

Figure 8. A comparison of the coda envelopes for the Model 4 synthetics (left) and observed explosion seismograms (right) for five narrow bands between 0.3 to 2 Hz.

CONCLUSIONS AND RECOMMENDATIONS

Our objective is to try to develop synthetic seismograms for *S*-wave coda from explosions. The ability to accurately model direct *Lg* and *Lg* coda using accurate earth models (both velocity and attenuation) will be important for regions in which explosion calibration data do not exist. Our results for NTS suggest we can numerically model direct *Lg* and *Lg* coda that have similar attenuation and propagation characteristics as observed data. We can do so using literature-based velocity and attenuation models and standard estimates for correlation lengths. We also have modeled explosion-generated coda that have attributes such as peak frequency and relative amplitudes that sometimes closely match observed nuclear explosion data, especially for the early onset arrivals in the coda windows.

Currently, our models do not produce realistic estimates of the frequency dependence for *Lg* coda in the Basin and Range. Aki (1969) described the coda as the result of backscattered waves from numerous heterogeneities distributed randomly and uniformly in the crust and upper mantle within an ellipse. Based on his definition, the scattering that creates the coda is from 3D phenomena; this suggests our initial modeling in 2D may never provide us with a perfect match between observed and synthetic coda. In order to achieve a model where the synthetic coda matches the observed, we may have to consider 3D models; however, this will ultimately either increase the computation time greatly or decrease the resolvable frequency bandwidth to below 1 Hz. Example synthetics for *Lg* and *Lg* coda from our first attempts at incorporating 3D stochastic models are shown in Figure 9.

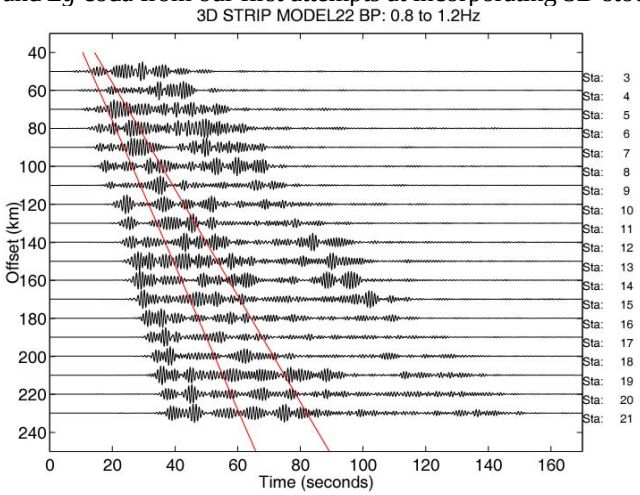

Figure 9. GFM synthetics in a 3D stochastic velocity model. The *Lg* group velocity window is outlined using the red lines.

REFERENCES

Aki, K. (1969). Analysis of seismic coda of local earthquake as scattered waves, *J. Geophys. Res*. 74: 615–631.

Aleqabi, G.I. and M.E. Wysession (2006). Q_{Lg} distribution in the Basin and Range province of the western United States. *Bull. Seism. Soc. Am*. 96: 384–354.

Baqer, S., and B. J. Mitchell (1998). Regional variation of *Lg* coda *Q* in the continental United States and its relation to crustal structure and evolution, *Pure Appl. Geophys.* 153: 613–638.

Benz, H. M., Unger, J. D., Leith, W. and V. Ryaboy (1991). The Norilsk DSS Profile in Northern Siberia: Interpretation of the velocity structure and comparison with Basin and Range and New England profiling results, Abstracts of the 13th Annual PL/DARPA Seismic Research Symposium: 85–100.

Benz, H. M., A. Frankel, and D. M. Boore (1997). Regional *Lg* attenuation for the continental United States, *Bull. Seism. Soc. Am.* 87: 606–619.

Bonner, J. L., K. Priestley, I. Tibuleac, and A. Stroujkova (2007). Estimating *Lg* coda Q on synthetic seismograms, Abs. *Seism. Res. Letts.* 78: 307.

Chavez, D. E., and K. F. Priestley (1986). Measurement of frequency dependent *Lg* attenuation in the Great Basin, *Geophys. Res. Lett.* 13**:** 551–554.

Ferguson, J.F., A.H. Cogbill, and R.G. Warren (1994). A geophysical-geological transect of the Silent Canyon caldera complex, Pahute Mesa, Nevada, *J. Geophys. Res.* 99: 4323–4339.

McLaughlin, K.L, L. R. Johnson, and T.V. McEvilly (1983). Two-dimensional array measurements of near-source ground accelerations. *Bull. Seism. Soc. Am.* 73: 349–375.

Mitchell, B.J., and J. Xie (1994). Attenuation of multiphase surface waves in the Basin and Range province, part III: Inversion for crustal anelasticity, *J. Geophys. Int*. 116: 468 -484.

Mitra, S. K. Priestley, V.K. Gaur, and S.S. Rai (2006). Frequency-dependent *Lg* attenuation in the Indian platform, *Bull. Seism. Soc. Am*. 96: 2449 -2456.

Murphy**,** K. R., K. Mayeda**,** and W. R. Walter (in review). Coda Spectral Peaking for Nevada Nuclear Test Site Explosions, submitted to *Seism. Soc. Am.*

Orrey, J. L. (1995). A generalized Fourier pseudospectral method for elastodynamics . Ph. D. Thesis. University of Colorado, Boulder.

Patton, H. J. and S. R. Taylor (1984). Q structure of the Basin and Range from surface waves, *J. Geophys. Res.* 89: 6929–6940

Singh, S. K., and R. B. Herrmann (1983). Regionalization of crustal coda *Q* in the continental United States, *J. Geophys. Res.* 88**:** 527–538.

Stevens, J. L., T. G. Berker, S. M. Day, K. L. McLaughlin, N. Rimer, and B. Shkoller (1991). Simulation of teleseismic body waves, regional seismograms, and Rayleigh wave phase shifts using two-dimensional, nonlinear models of explosion sources, *Explosion Source Phenomenology, Geophysical Monograph* 65: American Geophysical Union: 239–252.

Stump, B. W., and L. R. Johnson (1984). Near-field characterization of contained nuclear explosions in tuff, *Bull. Seism. Soc. Am.* 74: 1–26.

Tibuleac, I. M., A. Stroujkova, J. L. Bonner and K. Mayeda (2005). Predicting explosion generated *Lg* and *Sn* using synthetic seismograms, in *Proceedings of the 27th Seismic Research Review: Ground-Based Nuclear Explosion Monitoring Technologies*, LA-UR-05-6407, Vol. 1, pp. 214–221.

Tibuleac, I. M., A. Stroujkova, J. L. Bonner, K. Mayeda, and J. Britton (2006). Predicting explosion generated *Lg* and *Sn* using synthetic seismograms, in *Proceedings of the 28th Seismic Research Review: Ground-Based Nuclear Explosion Monitoring Technologies*, LA-UR-06-5471, Vol. 1, pp. 283–294.

Xie, J. and O. Nuttli (1988). Interpretation of high-frequency coda at large distance: stochastic modeling and method of inversion, *Geophys. J.* 95: 579–595

Xie, J., and B. J. Mitchell (1990). Attenuation of multiphase surface waves in the Basin and Range Province, part I, *Lg* and *Lg* coda, *Geophys. J. Int.* 102:121–137.